# Displacive mechanisms and order-parameter symmetries for the A7-incommensurate-bcc sequences of high-pressure reconstructive phase transitions in Group Va elements

Hannelore Katzke[1,*] and Pierre Tolédano[2]

[1]*Institute of Geosciences, Crystallography, University of Kiel, Olshausenstraße 40, 24098 Kiel, Germany*

[2]*Department of Physics, Faculty of Sciences, University of Picardie, 33 rue Saint-Leu, 80000 Amiens, France*

(Received 12 October 2007; revised manuscript received 7 December 2007; published 18 January 2008)

The high-pressure structural transitions observed in the Group Va elements P, As, Sb, and Bi are described by displacive atomic mechanisms. A theoretical analysis of the proposed mechanisms shows that two different structural paths are followed relating the low-pressure A7 structure to the highest-pressure bcc structure. One structural path gives rise to the host-guest structures found in As, Sb, and Bi, whereas another path yields the incommensurate P IV structure recently disclosed in P. The incommensurate character of the host-guest and P IV structures is shown to be imposed by the energetically most favorable path relating the A7 and bcc structures.

DOI: 10.1103/PhysRevB.77.024109 PACS number(s): 62.50.−p

## I. INTRODUCTION

The existence of similar host-guest structures in bismuth, antimony, and arsenic[1–3] and the incommensurate character recently reported for the P IV structure of phosphorus[4] suggest a systematic trend for the high-pressure phase diagram of Group Va elements. With the exception of molecular nitrogen, which follows a different structural scheme,[5] the sequences of high-pressure transitions in Group Va, shown in Fig. 1, reveal indeed a number of common features but also some differences. In As, Sb, and Bi, the host-guest structures take place between the A7 room-pressure phase and the bcc phase attained at the highest pressure applied. Primitive cubic or monoclinic structures separate the A7 and host-guest structures in As and Bi, whereas in Sb, the A7-to-host-guest transition is direct. In P, the A7-to-primitive cubic transition occurs above the room-pressure A17 structure of black phosphorus, then undergoes a sequence of incommensurate-to-primitive hexagonal transitions before the onset of the bcc phase. A regular decrease with increasing atomic weight is observed for the critical pressures giving rise to the bcc phase: 262 GPa for P, 97 GPa for As, 28 GPa for Sb, and 7.7 GPa for Bi. The same decrease is found for the stability of the A7 structure in As, Sb, and Bi which extends, respectively, up to 25, 8, and 2.55 GPa.

Host-guest structures with an apparent structural similarity than in Group Va have been disclosed in elements of Group Ia (Rb, K),[6,7] Group IIa (Sr, Ba),[8,9] and in the transition metal Sc.[10] At the electronic level, the formation of these composite incommensurate structures at high pressure was interpreted as resulting from an increasing *d* occupancy of the electronic shell, the host and guest atoms being more *s*- and *d*-like, respectively.[11] Since in elements of Group Va such differentiation cannot be invoked, it has been suggested[12] that the host-guest structures in As, Sb, and Bi would be the consequence of an interplay between the band and electrostatic Madelung energies. We have recently proposed[13] that the electronic frustration leading to the formation of host-guest structures in Sr and Ba was reflected at the structural level in a competition between Burgers (bcc → hcp) and Bain (bcc → fcc) transition mechanisms. In Rb and K, the onset of host-guest structures was also shown to be at the crossover of competing structural mechanisms,[14] representing a crystallographic counterpart to the *s-d* electron transfer: Bain mechanism dominates the lower pressure region of alkali metals, being interrupted by a lock-in mechanism which gives rise to the intermediate *Cmca*−Rb VI structure, on the way to the high-pressure double-hcp structure of Cs VI.

In the present work, we first describe in terms of critical displacements and strains the transition mechanisms taking place at high pressure in elements of Group Va (Sec. II). When pure symmetry and geometrical arguments are considered, a number of different transition paths can be *a priori* proposed. However, when taking into account (1) the shortest set of displacements relating the initial and final real atomic positions, assuming implicitly a minimal energy principle for the actual transition mechanism, (2) the orientational relationship between neighboring structures, and (3) the overall consistency of the successive set of displacements in a given element, then the possible transition path is found to be, in most cases, unique. A theoretical analysis of the assumed mechanisms is then made in the framework of the Landau theory of reconstructive phase transitions[15] (Sec. III). It shows that despite the apparent structural similarities with the host-guest structures of Groups Ia and IIa, the host-guest

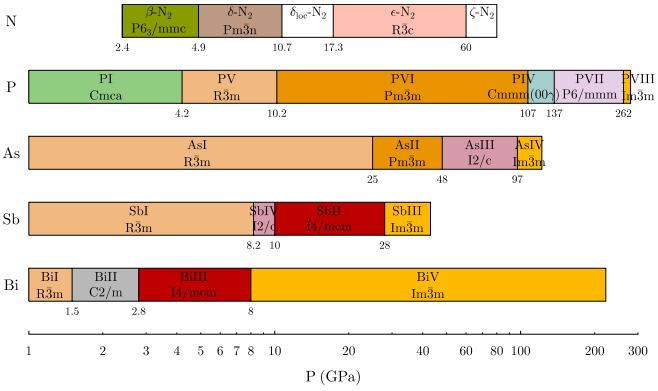


FIG. 1. (Color online) Symmetry of the high-pressure phases in Group Va elements.

 

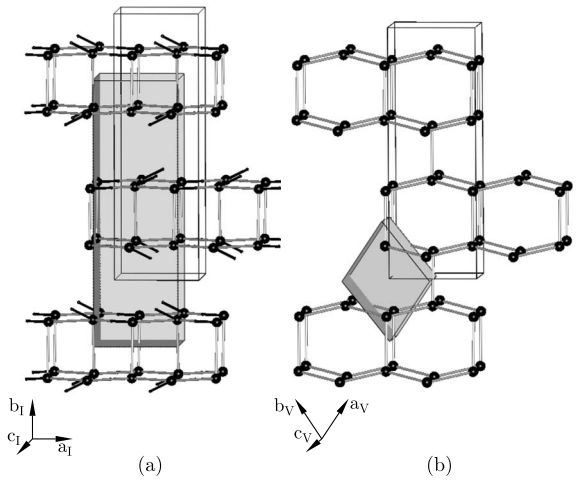


FIG. 2. Structural relationship between P I and P V. (a) Orthorhombic *Cmca* structure of the thermodynamically stable modification of black phosphorus. The A17-to-A7 structural transition can be described as proceeding via a common $P2/c$ ($Z=8$) structure with the phosphorus atoms occupying two Wyckoff positions $4g$ (0.0806, 0.7500, 0.8534) and (0.4194, 0.2500, 0.8534) in P I and (0.0700, 0.5000, 0.8925) and (0.4300, 0.0000, 0.8575) in P V, respectively. Therefore, the A17 structure of P I is transformed into the A7 structure of P V by antiparallel displacements of adjacent (010) layers by $\pm 1/4$ [100], indicated by black arrows of the real magnitude, and a shear deformation decreasing the monoclinic angle $\beta$ of the common $P2/c$ substructure from 90° to 86.62°. The orthorhombic unit cell is shown as a gray polyhedron; the monoclinic $P2/c$ unit cell of the common substructure is shown by solid lines. The origin of the $P2/c$ unit cell is shifted to $p=(1/4,1/4,0)$. (b) Rhombohedral $R\bar{3}m$ structure of P V. The rhombohedral unit cell is shown as a gray polyhedron; the monoclinic unit cell of the common substructure is shown by solid lines. The origin of the $P2/c$ unit cell is shifted to $p=(1/2,1/2,1/2)$.

structures found in As, Sb, and Bi and the incommensurate P IV structure can be interpreted by a different type of structural frustration occurring along the sequence of high-pressure transitions, in order to minimize the structural path between the A7 and bcc structures.

## II. STRUCTURAL TRANSITION MECHANISMS IN P, As, Sb, AND Bi

### A. Phosphorus

The critical displacements transforming the room-pressure A17 structure of black phosphorus P I (space group *Cmca*, with $Z=8$ atoms in the conventional unit cell)[16] into the A7 rhombohedral structure of P V ($R\bar{3}m$, $Z=2$) (Ref. 17) are shown in Fig. 2. The transition, which is strongly first order, occurs at about 4.2 GPa. It has a reconstructive character with no direct group-subgroup relationship between the P I and P V symmetries. As it is usual for reconstructive transitions,[15] it can be described as proceeding via a common substructure with monoclinic symmetry ($P2/c$, $Z=8$) shown in Fig. 2. An alternative description of the P I→P V mechanism can be proposed by considering that both the P I and P V structures contain as building units six-membered rings in the chair conformation, stacked along [012] in P I and along [111] in P V, similar to the $C_6$ rings of the diamond-type structure ($Fd\bar{3}m$, $Z=8$), which is the room-pressure parent structure of the neighboring Group IVa elements Si and Ge.[18] Accordingly, it is reasonable to assume that the P I and P V structures both derive from a latent diamond-type structure. Figures 3(a) and 3(b) show the structural paths and critical displacements associated with the diamond-to-P I and diamond-to-P V transformations. The diamond-to-P I transition proceeds via a common orthorhombic structure (*Pbam*, $Z=8$), the diamond-type and A7 structures being group-subgroup related. Another possible structural path, suggested in previous works,[19,20] is the formation of the A17 and A7 structures from a parent primitive cubic structure. It is shown in Fig. 4. The simple cubic-to-P I transition can be described as proceeding via a common orthorhombic substructure (*Pbcn*, $Z=8$).

At 10.2 GPa, P V undergoes a symmetry increase to the primitive cubic P VI structure,[21] to which it is group-subgroup related. The transition involves small antiparallel displacements of $\pm 0.035$ along the [111] cubic direction, with an increase of the rhombohedral angle from 57.262° to 60°. Figure 5 shows the connection between the P V and P VI structures.

P VI remains stable up to 107 GPa where it transforms discontinuously into P IV,[21] which in turn undergoes at 137 GPa a first-order transition to the simple hexagonal structure ($P6/mmm$, $Z=1$) (Ref. 22) of P VII. The intermediate P IV structure has been the subject of a number of speculations[23–25] before being identified as an incommensurately modulated structure[4] accurately fitted with the orthorhombic superspace group $Cmmm(00\gamma)s00$. With increasing pressure, $\gamma$ slightly decreases from 0.268 to 0.266, the angle between the diagonals of the cube increasing from 90° to 97.8° at the first-order P VI→P IV transition and from 97.8° to 120° at the P IV→P VII transition. The basic structure of P IV has the symmetry *Cmmm* with two atoms in position $2a$.[4] It coincides with the maximal substructure common to the P VI and P VII structures. Therefore, P IV appears as an intermediate stage in the reconstructive mechanism transforming the primitive cubic into the primitive hexagonal structure, which is represented in Fig. 6. At the P VI→P IV transition, a transverse modulation wave arises running along the $c$ axis and displacing the atoms along the cubic [110] direction by maximal 0.41 Å. The modulation vanishes at the P IV→P VII transition at 137 GPa.

The P VII structure, also found at high pressure in the Group IVa elements Si and Ge,[18] preserves its stability up to extremely high pressures, before transforming at 262 GPa into the P VIII bcc structure.[26] Figure 7 shows the structural relationship between P VII and P VIII. The corresponding reconstructive structural path goes through a monoclinic substructure ($C2/m$, $Z=2$), common to P VII and P VIII with the phosphorus atoms occupying the special position $2a$. Hence, the P VII→P VIII transition involves only strain increasing the monoclinic angle $\beta$ from 90° in P VII to 125.264° in P VIII.

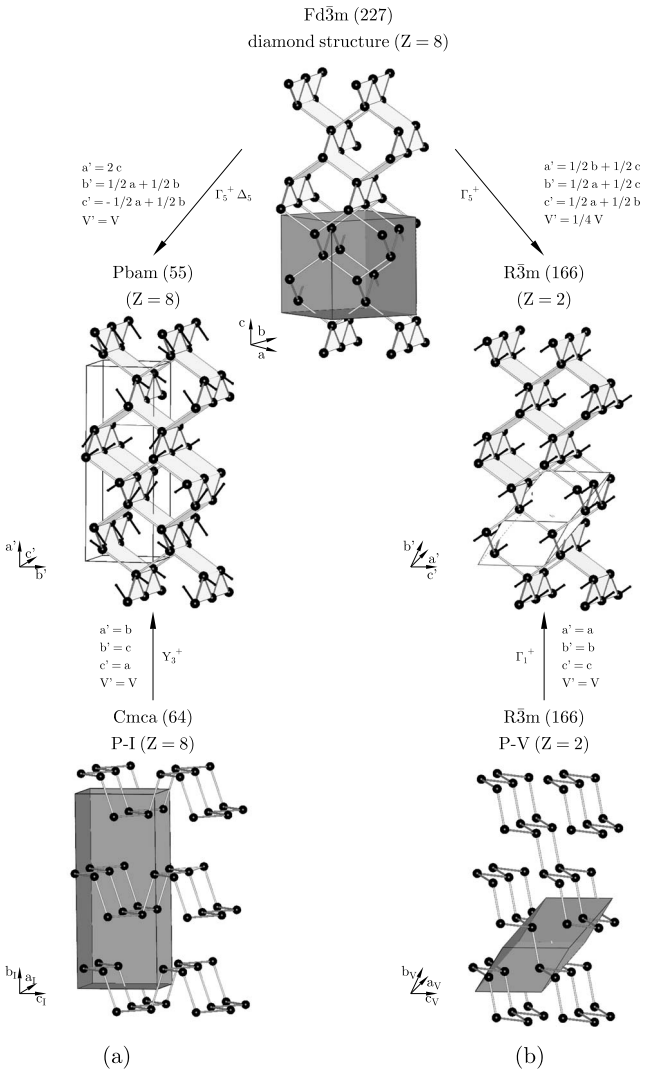


FIG. 3. (a) Structural relationship between the orthorhombic A17 structure of black phosphorus and the diamond structure. The diamond-to-P I transition can be described as proceeding via a common orthorhombic substructure (*Pbam*, $Z$=8) with the phosphorus atoms occupying the Wyckoff positions 4*g* (0.0625, 0.2500, 0) and 4*h* (0.1875, 0.2500, 1/2) in the diamond-type structure and 4*g* (0.1034, 0.0806, 0) and 4*h* (0.1034, 0.4194, 1/2) in the structure of P I. The diamond-type-to-P I transition involves antiparallel displacements of the phosphorus atoms in the $a/b$ plane corresponding to the $b/c$ plane of P I, indicated by black arrows. The cubic $Fd\bar{3}m$ and the orthorhombic *Cmca* unit cells of P I are shown as gray polyhedra. The *Pbam* unit cell of the common substructure is shown by solid lines. (b) Structural relationship between the diamond structure and the A7 rhombohedral structure of P V. The diamond structure is transformed into the P V structure by antiparallel displacements of $\pm 0.09[111]$ and a shear deformation decreasing the rhombohedral angle $\alpha$ from 60° to 57.262°.

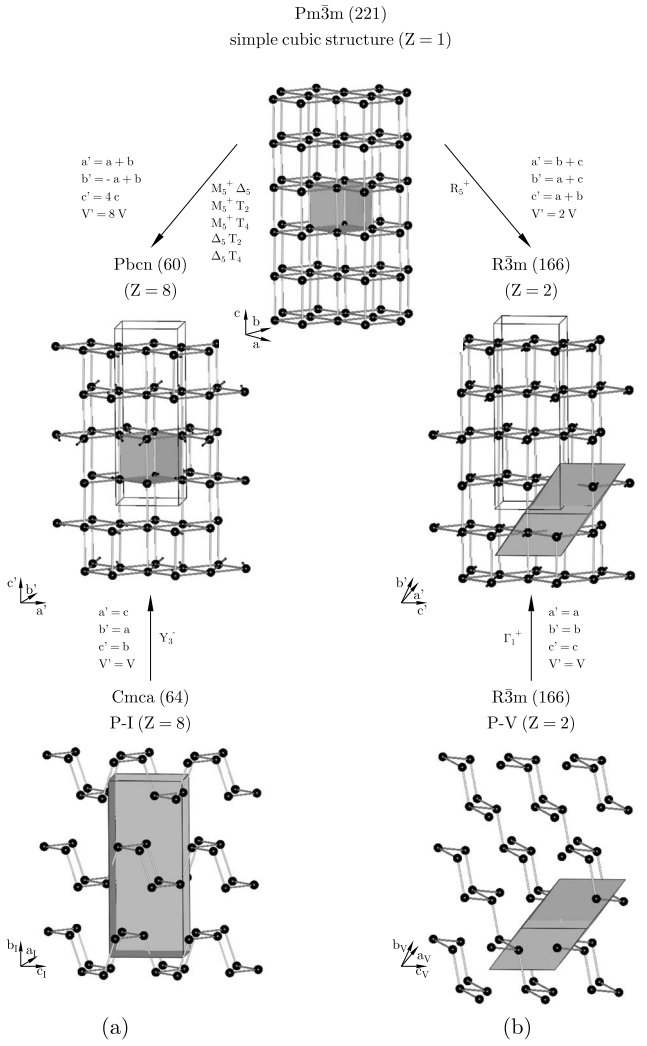


FIG. 4. (a) Structural relationship between the orthorhombic A17 structure of black phosphorus and the simple cubic structure. The simple cubic-to-P I transition can be described as proceeding via a common orthorhombic substructure (*Pbcn*, $Z$=8) with the phosphorus atoms occupying the Wyckoff position 8*d* (0,1/2,7/8) in the simple cubic structure and 8*d* (0.0806, 3/4, 0.8534) in P I. The displacements of the atoms are indicated by black arrows. The cubic $Pm\bar{3}m$ and the orthorhombic *Cmca* unit cell are shown as gray polyhedra. The *Pbcn* unit cell of the common substructure is shown by solid lines. (b) Structural relationship between the simple cubic structure and the A7 rhombohedral structure of P V. The simple cubic structure is transformed into the P V structure by antiparallel displacements of $\pm 0.035[111]$ and a shear deformation decreasing the rhombohedral angle $\alpha$ from 60° to 57.262°.

### B. Arsenic

The rhombohedral-to-primitive cubic As I→As II transition[27] differs from the P V→P VI transition (Fig. 5), only by the value of the rhombohedral angle $\alpha$, which increases steadily from 54.13° to 59° before adopting the cubic value $\alpha$=60°. The transition takes place discontinuously at 25 GPa, with a drop in volume smaller than 0.5% and hysteresis less than 2 GPa. This is in contrast with the sluggish character of the As II→As III transition which extends from 42 to 53 GPa.[28] The host-guest structure of As III (Refs. 2 and 28) comprises a body-centered monoclinic host ($I2/c$, $Z$=8) and a body-centered monoclinic guest ($I2/m$, $Z$=2) with 10.61 atoms in the unit cell of the resulting host-guest structure. The monoclinic symmetry implies that the guest atoms are modulated along both the common $c$ axis and $a/b$

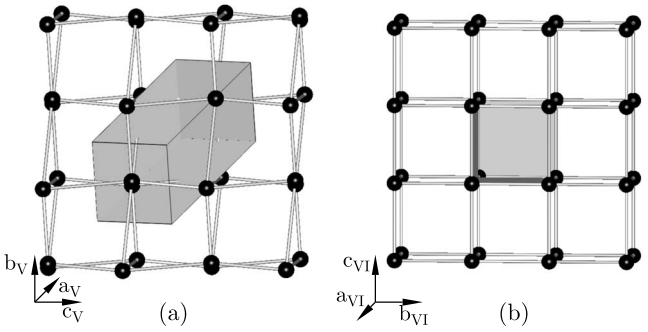


FIG. 5. Structural relationship between (a) P V and (b) P VI. The P V→P VI phase transition is associated with small atomic displacements of the phosphorus atoms of ±0.035 along the [111] direction. The rhombohedral unit cell of P V and the cubic unit cell of P VI are shown as gray polyhedra in (a) and (b), respectively.

plane of the host and guest structures. In the superspace formalism,[29] the host-guest structure is described[28] by the superspace group $I'2/c(q_1 0 q_3)00$, where $q_3=\frac{c_H}{c_G}=1.3047$ and $q_1=\frac{a_G \cos\beta_G - a_H \cos\beta_H}{c_G}=0.1162$. Figure 8(a) shows a projection in the $a/b$ plane of the calculated critical displacements of arsenic atoms, in the real magnitude, required to transform the primitive cubic As II structure into the As III host-guest structure [Fig. 8(b)]. Figure 9(a) represents the critical atomic displacements transforming the As III structure into the higher-pressure bcc As IV structure [Fig. 9(b)], which takes place at 97 GPa and remains stable up to at least 122 GPa.[30]

### C. Antimony

The Sb IV host-guest structure has been observed in a narrow interval of pressure, between 8.2 and 9 GPa on pressure increase and between 8 and 6.9 GPa on pressure decrease.[2] It is isostructural with As III and described by the same superspace group $I'2/c(q_1 0 q_3)00$ with $q_3=1.3132$ and $q_1=0.1662$ and 10.63 atoms in the unit cell. It is transformed directly from the rhombohedral Sb I structure[31] and not from a primitive cubic structure, as indicated in earlier works.[32] Figure 10 shows the relationship between the Sb I and Sb IV structures and the set of atomic displacements associated with the Sb I→Sb IV transition. With increasing pressure, Sb IV undergoes a slightly discontinuous transition to the host-guest Sb II structure,[1] with a further more strongly first-order transition to bcc Sb III at 28 GPa.[33]

The space groups of the host and guest structures composing Sb II are $I4/mcm$ and $I4/mmm$, respectively, with the same lattice parameter $a_H=a_G$ and a ratio $q_3=c_H/c_G$ decreasing slightly, from about 1.310 to 1.305, in the stability range of Sb II.[1,28] The superspace group of the composite structure is $I'4/mcm(00q_3)0000$. Sb II remains stable up to 65 GPa,[28,33] where it transforms to bcc Sb III.

### D. Bismuth

The room-pressure A7 structure of Bi transforms discontinuously at 2.55 GPa into the monoclinic structure of Bi II

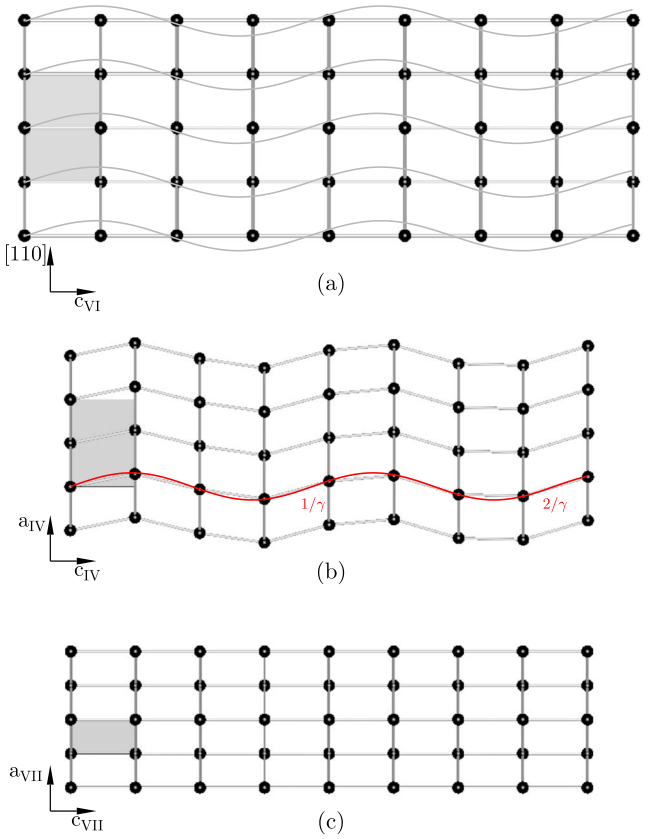


FIG. 6. (Color online) Structural relationship between the primitive cubic structure of P VI, the incommensurate structure of P IV, and the primitive hexagonal structure of P VII. (a) Primitive cubic structure of P VI, projected along $[\bar{1}10]$. The cubic unit cell is shown as a gray polyhedron; the orthorhombic *Cmmm* unit cell of the common substructure is shown by solid lines. The superimposed modulation wave (gray lines) represents the real displacements of the phosphorus atoms along [110] occurring at the P VI→P IV transition. (b) Projection of the incommensurate structure of P IV along [010]. The transverse modulation wave is running along the *c* axis with a displacement of the atoms along the *a* axis. The orthorhombic unit cell of the basic structure is shown as a gray polyhedron. (c) Primitive hexagonal structure of P VII, projected along [120]. The hexagonal unit cell is shown as a gray polyhedron.

$(C2/m, Z=4)$,[34,35] which is unique among elements. The two structures are not group-subgroup related and the corresponding transition mechanism has a strong reconstructive character. The transformation mechanism can be best described as proceeding via a common primitive cubic superstructure to which the space groups of the rhombohedral Bi I and monoclinic Bi II structures are group-subgroup related. Whereas Bi I has a slightly distorted primitive cubic structure, the Bi II structure can be described as a heavily distorted primitive cubic array.[36] Figure 11 shows the set of atomic displacements occurring at the primitive cubic-to-Bi II transition. It involves antiparallel displacements of the bismuth atoms by ±0.149[001], corresponding to the [101] direction in the cubic unit cell, and a shear deformation decreasing the monoclinic angle $\beta$ from 135.0° in the primitive cubic structure to 110.412° in Bi II.

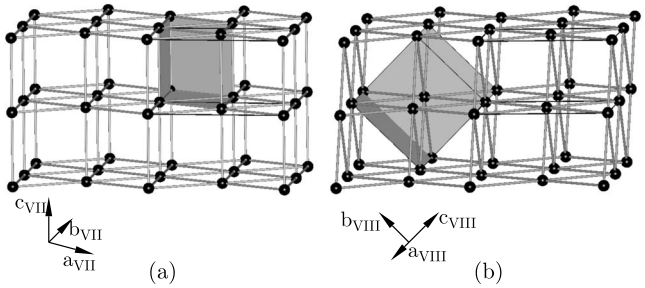


FIG. 7. Structural relationship between P VII and P VIII. The P VII→P VIII transition can be described as proceeding via a common monoclinic substructure ($C2/m, Z=2$). (a) Primitive hexagonal structure of P VII. The hexagonal unit cell is shown as a gray polyhedron; the monoclinic unit cell of the common $C2/m$ substructure is shown by solid lines. The P VII→P VIII transition involves a large monoclinic deformation, increasing the monoclinic angle $\beta$ from 90° in P VII to 125.264° in P VIII. (b) Cubic body-centered structure of P VIII. The cubic unit cell is shown as a gray polyhedron; the monoclinic unit cell is represented by solid lines.

Bi II has a very narrow pressure stability range and transforms into the host-guest Bi III structure at 2.8 GPa.[1] Below about 200 K, Bi II disappears and Bi I transforms directly into Bi III.[37] The Bi III structure is isostructural to Sb II,[1] i.e., it comprises tetragonal host and guest structures, the interpenetrating guest component being incommensurate with the host along the tetragonal $c$ axis, with $c_H/c_G$ decreasing slightly with pressure from 1.311 at 3 GPa to 1.309 at 8.5 GPa. This ratio is very close to the Sb II ratio and the number of atoms in the host structure is therefore the same for the two elements (10.62). The Bi II→Bi III transition is first order with a volume drop of about 3.5%.[28] Figure 12 shows the relationship between the corresponding monoclinic and tetragonal structures and the critical displacements transforming Bi II into Bi III. At 7.7 GPa, Bi III transforms into bcc Bi V (Ref. 38) with a small volume drop of about 1%.[28] Bi V remains stable up to 222 GPa.[39] The

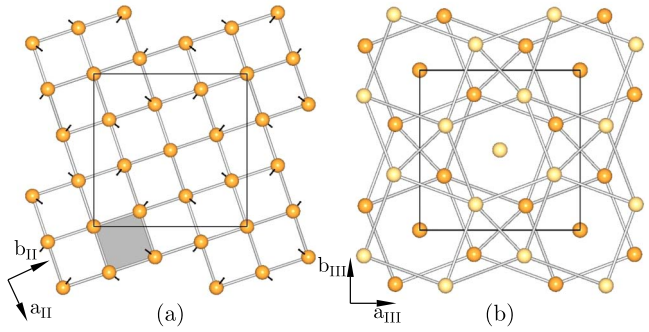


FIG. 8. (Color online) Displacive mechanism associated with the As II→As III phase transition. (a) Primitive cubic structure of As II, projected along [001]. The cubic unit cell is shown as a gray polyhedron; the As III-related unit cell with its origin shifted to $p=(0,0,-1/4)$ is represented by solid lines. The arrows indicate the atomic displacements associated with the structural phase transition. (b) Host-guest structure of As III, projected along [001]. Atoms on different heights along $c$ are shown in different gray shades (colors).

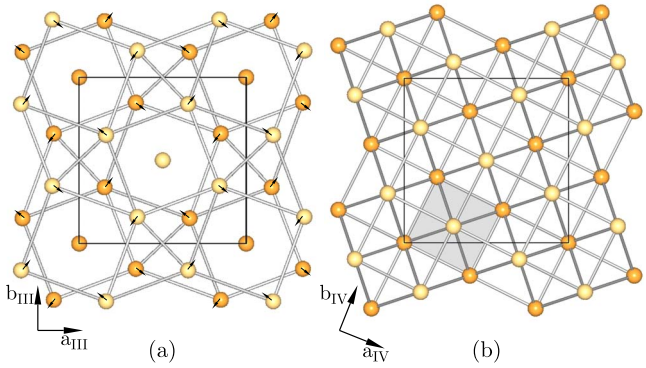


FIG. 9. (Color online) Displacive mechanism associated with the As III→As IV phase transition. (a) Host-guest structure of As III, projected along [001]. Atoms on different heights along $c$ are shown in different gray shades (colors). The arrows indicate the atomic displacements associated with the structural phase transition. (b) Body-centered cubic structure of As IV. The cubic unit cell is shown as a gray polyhedron, whereas the As III-related unit cell is shown by solid lines.

Bi III→Bi V transition mechanism, similar to Sb II→Sb III and As III→As IV, is illustrated in Fig. 9.

Another confirmed high-pressure phase exists in bismuth below the melt, which occupies the triangular-shaped region above Bi III and between the low-pressure Bi II and higher-pressure Bi V structures. It is denoted Bi IV by Chen *et al.*[40] who assigned a $P2_1/n$ ($Z=8$) symmetry to its structure before it was reinterpreted as having the orthorhombic $Cmca$ ($Z=16$) symmetry,[41] similar to the Si VI and Ge VI structures.[18] Figure 13 shows the relationship between Bi II and Bi IV and the displacements transforming Bi II into Bi IV via an intermediate common substructure with monoclinic symmetry $C2/c$ ($Z=16$). Note that although Bi IV transforms at high pressure into bcc Bi V, it can be more consistently interpreted as a distorted fcc structure with $c/a>1$ than a distorted bcc structure. The structural relationship between Bi IV and the fcc structure is shown in Fig. 14.

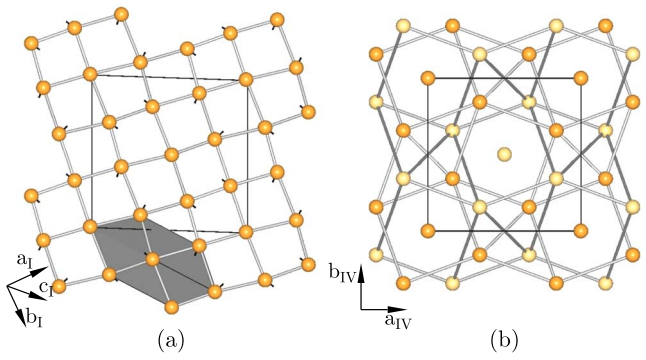


FIG. 10. (Color online) Displacive mechanism associated with the Sb I→Sb IV phase transition. (a) Rhombohedral A7 structure of Sb I, projected along $[11\bar{1}]$. The rhombohedral unit cell is shown as a gray polyhedron. The arrows indicate the atomic displacements associated with the structural phase transition. (b) Host-guest structure of Sb IV, projected along [001]. Atoms on different heights along $c$ are shown in different gray shades (colors).

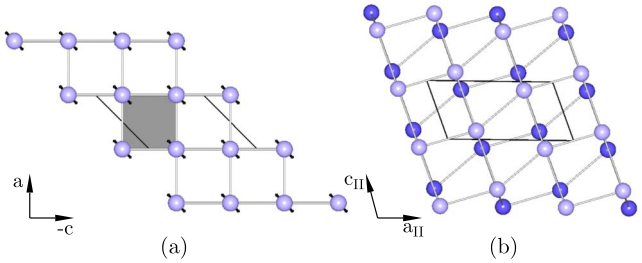


FIG. 11. (Color online) (a) Projection of the primitive cubic structure along [010], showing the set of atomic displacements taking place at the primitive cubic-to-Bi II phase transition. The cubic unit cell is shown as a gray polyhedron; the monoclinic $C2/m$ unit cell with its origin shifted to $p=(0,0,-1/2)$ is represented by solid lines. (b) Monoclinic structure of Bi II, projected along [010]. Atoms on different heights along $b$ are shown in different gray shades (colors).

## III. THEORETICAL ANALYSIS AND DISCUSSION

### A. Landau symmetry analysis

Table I summarizes the structural properties involved in the transition mechanisms assumed for P, As, Sb, and Bi and the corresponding symmetry-breaking order parameters and macroscopic strains deduced from a Landau symmetry analysis. The symmetry relationships between the different high-pressure structures are shown in Fig. 15. It reveals that with the exception of the A7-to-primitive cubic (pc) transition, all the high-pressure phase transitions in the four considered elements are of the reconstructive type and proceed indirectly via common substructures or superstructures which have been disclosed in the displacive mechanisms described in Sec. II. A theoretical analysis of these mechanisms should help clarifying the main questions posed by the observed sequences of structural transitions in Group Va elements, namely, why host-guest structures with similar structural features take place in As, Sb, and Bi between the A7 and bcc structures? Why phosphorus, which also displays the low-pressure A7 and higher-pressure bcc structures, follows a different intermediate structural path?

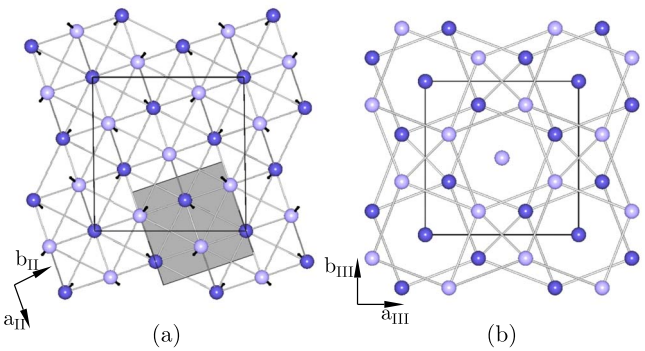


FIG. 12. (Color online) Structural relationship between Bi II and Bi III. (a) Monoclinic structure of Bi II, projected along [001]. The atomic displacements transforming Bi II into Bi III are indicated by arrows. The monoclinic $C2/m$ unit cell of Bi II, projected along [001], is shown as a gray polyhedron; the Bi III-related unit cell, with the origin shifted to $p=(1/4,-1/2,1/4)$ is represented by solid lines. (b) Host-guest structure of Bi III, projected along [001]. Atoms on different heights along $c$ are shown in different gray shades (colors).

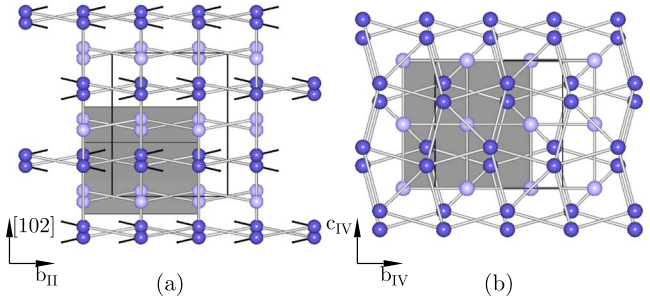


FIG. 13. (Color online) Structural relationship between Bi II and Bi IV. (a) Monoclinic structure of Bi II, projected along $[10\bar{2}]$. The Bi II→Bi IV transition can be described as proceeding via a common monoclinic substructure ($C2/c, Z=16$) with the bismuth atoms occupying two Wyckoff positions $8f$ (0.4637, 0.25000, 0.0382) and (0.2864, 0.2500, 0.7119) in Bi II and (0.4602, 0.2500, 0.0000) and (0.2500, 0.0667, 0.6775) in Bi IV. The atomic displacements are indicated by black arrows. The monoclinic $C2/m$ unit cell of Bi II is shown as a gray polyhedron; the monoclinic $C2/c$ unit cell of the common substructure is shown by solid lines. The origin of the $C2/c$ cell is shifted to $p=(-3/4,1/4,0)$. (b) Orthorhombic structure of Bi IV, projected along [100]. The orthorhombic unit cell is shown as a gray polyhedron; the monoclinic unit cell of the common substructure, with the origin shifted to $p=(1/4,-1/4,0)$ is represented by solid lines. Atoms on different heights along $[10\bar{2}]$ in (a) and [100] in (b) are shown in different gray shades (colors).

The A7 structure corresponds to a small distortion of the parent pc structure, induced by the three-dimensional irreducible representation (IR) $R_5^+$ at the $R$-corner point of the pc Brillouin zone,[42] with equilibrium values $\eta_1=\eta_2=\eta_3$ of the displacive order-parameter components. The associated spontaneous shear strain $e_{yz}=e_{xz}=e_{xy}$ plays the role of a sec-

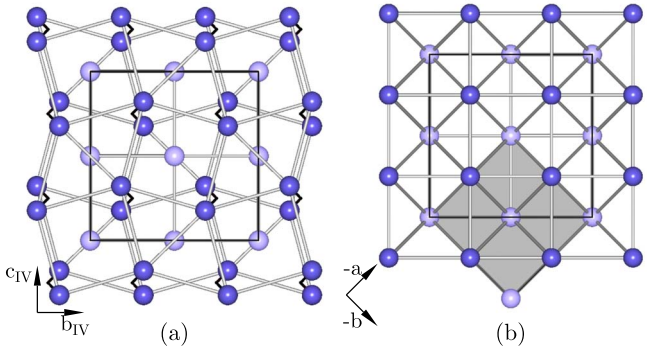


FIG. 14. (Color online) Structural relationship between Bi IV and a face-centered cubic structure. (a) Structure of Bi IV, projected along [100]. The atomic displacements transforming Bi II into a distorted fcc structure are shown by black arrows. (b) Face-centered cubic structure, projected along $[00\bar{1}]$. The cubic unit cell is shown as a gray polyhedron, whereas the orthorhombic $Cmca$ unit cell is shown by solid lines. The origin of the $Cmca$ unit cell is shifted to $p=(0,0,1/2)$. Atoms on different heights along [100] in (a) and [001] in (b) are shown in different gray shades (colors).

TABLE I. Structural changes and order-parameter symmetries for the transitions in Group Va. The columns have the following meaning. (a) Space-group changes and number of atoms in the primitive unit cells for the transitions in P, As, Sb, and Bi indicated in column (b). The empty squares in this column symbolize hypothetical structures used in the assumed transition mechanisms. (c) Relationships between the basic vectors of the final and initial conventional unit cells. (d) Multiplication of the number of atoms in the primitive unit cell. (e) Irreducible representations (IRs) inducing the transitions and corresponding critical wave vectors in the Brillouin zone of the initial structure, using the notations indicated in Ref. 42. (f) Dimension of the IRs and of the order parameters. (g) Equilibrium values of the order-parameter components ($\eta_i$) in the final structure. (g) Secondary strain components ($e_{ij}$) involved at the transition. The full notation of the superspace groups $I'4/mcm$ and $I'2/c$ is given in the text.

| (a) | (b) | (c) | (d) | (e) | (f) | (g) | (h) |
|---|---|---|---|---|---|---|---|
| $Pm\bar{3}m(1)\rightarrow R\bar{3}m(2)$ | P VI→P V, As II→As I | **b**+**c**, **a**+**c**, **a**+**b** | 2 | $R_5^+\ (\frac{\pi}{a},\frac{\pi}{a},\frac{\pi}{a})$ | 3 | $\eta_1=\eta_2=\eta_3$ | $e_{xz}=e_{yz}=e_{xy}$ |
| $Pm\bar{3}m(1)\rightarrow Cmmm(1)$ | P VI→P IV | **a**+**b**, **b**−**a**, **c** | 2 | $\Delta\ (0,0,k_z)$ | 4 | $\eta_1=\eta_3$, $\eta_2=\eta_4=0$ | $e_{xy}$ |
| $P6/mmm(1)\rightarrow Cmmm(1)$ | P VII→P IV | **a**, **a**+2**b**, **c** | 1 | $\Delta\ (0,0,k_z)$ | 4 | $\eta_1=\eta_4$, $\eta_2=\eta_3=0$ | $e_{xx}-e_{yy}$ |
| $P6/mmm(1)\rightarrow C2/m(1)$ | P VII→P VIII | −**b**, 2**a**+**b**, **c** | 1 | $\Gamma_6^+\ (0,0,0)$ | 2 | $e_{yz}$, $e_{xz}=0$ | $e_{xx}-e_{yy}$ |
| $Im\bar{3}m(1)\rightarrow C2/m(1)$ | P VIII→P VII | −**c**, −(**a**+**b**), $\frac{1}{2}$ (**b**+**c**−**a**) | 1 | $\Gamma_4^+\ (0,0,0)$ | 3 | $e_{xz}=e_{yz}$, $e_{xy}=0$ | $e_{xy}$, $2e_{zz}-e_{xx}-e_{yy}$ |
| $Pm\bar{3}m(1)\rightarrow I'2/c(5.3)$ | As II→As III | **a**+3**b**, **b**−3**a**, **c** | 5.3 | $\Sigma_1\ (\frac{\pi}{5a},\frac{\pi}{5a},0)$ +$\Delta\ (0,0,k_z)$ | 24 | $\eta_1=\eta_2$, $\eta_{3\rightarrow 24}=0$ | $e_{xy}$, $2e_{zz}-e_{xx}-e_{yy}$ |
| | | | | | 12 | $\rho_1=\rho_2$, $\rho_{3\rightarrow 12}=0$ | |
| $Im\bar{3}m(1)\rightarrow I'2/c(5.3)$ | As IV→As III | 2**a**+**b**, 2**b**−**a**, **c** | 5.3 | $\Sigma_1\ (\frac{2\pi}{5a},\frac{2\pi}{5a},0)$ +$\Delta\ (0,0,k_z)$ | 24 | $\eta_1=\eta_2$, $\eta_{3\rightarrow 24}=0$ | $e_{xy}$, $2e_{zz}-e_{xx}-e_{yy}$ |
| | | | | | 12 | $\rho_1=\rho_2$, $\rho_{3\rightarrow 12}=0$ | |
| $Im\bar{3}m(1)\rightarrow I'4/mcm(5.3)$ | Sb III→Sb II, Bi V→Bi III | 2**a**+**b**, 2**b**−**a**, **c** | 5.3 | $\Sigma_1\ (\frac{2\pi}{5a},\frac{2\pi}{5a},0)$ +$\Delta\ (0,0,k_z)$ | 24 | $\eta_1=\eta_2$, $\eta_{3\rightarrow 24}=0$ | $2e_{zz}-e_{xx}-e_{yy}$ |
| | | | | | 12 | $\rho_1=\rho_2$, $\rho_{3\rightarrow 12}=0$ | |
| $R\bar{3}m(2)\rightarrow I'2/c(5.3)$ | Sb I→Sb IV | **a**−**b**+2**c**, 2**a**−2**b**−**c**, $\frac{1}{2}$ (**a**+**b**−**c**) | 5.3 | $\Sigma_1\ (\frac{2\pi}{7a},\frac{2\pi}{7a},0)$ +$\Delta\ (0,0,k_z)$ | 4 | $\eta_1=\eta_2$, $\eta_3=\eta_4=0$ | $e_{yz}$, $e_{xx}-e_{yy}$ |
| | | | | | 4 | $\rho_1=\rho_2$, $\rho_3=\rho_4=0$ | |
| $C2/m(2)\rightarrow I'4/mcm(5.3)$ | Bi II→Bi III | $\frac{1}{2}$ (**a**+3**b**), $\frac{1}{2}$ (**b**−3**a**), **c** | $\frac{5.3}{2}$ | $\Sigma_1\ (\frac{2\pi}{5a},\frac{2\pi}{5a},0)$ +$\Delta\ (0,0,k_z)$ | 2<br>2 | $\eta_1=\eta_2$<br>$\rho_1=\rho_2$ | $e_{yz}=-e_{xz}$ |
| $I'4/mcm(5.3)\rightarrow I'2/c(5.3)$ | Sb II→Sb IV | **a**, **b**, **c** | 1 | $\Gamma_5^+\ (0,0,0)$ | 2 | $e_{yz}=-e_{xz}$ | $e_{xy}$ |
| $Pm\bar{3}m(1)\rightarrow C2/m(2)$ | □→Bi II | −2**c**, 2**b**, **a**+**c** | 2 | $R_5^-\ (\frac{\pi}{a},\frac{\pi}{a},\frac{\pi}{a})$ | 3 | $\eta_1=\eta_2=\eta_3$ | $e_{xy}$<br>$2e_{zz}-e_{xx}-e_{yy}$ |
| $C2/m(2)\rightarrow C2/c(8)$ | Bi II→□ | **a**−2**c**, **b**, **a**+2**c** | 4 | $X_1\ (\frac{\pi}{a},0,0)$ +$\Delta\ (0,0,\frac{\pi}{2a})$ | 2 | $\eta_1=\eta_2$ | |
| $Cmca(8)\rightarrow C2/c(8)$ | Bi IV→□ | **a**, **b**, **c** | 1 | $\Gamma_4^+\ (0,0,0)$ | 1 | $e_{xz}$ | |
| $Fd\bar{3}m(2)\rightarrow R\bar{3}m(2)$ | □→P V | $\frac{1}{2}$ (**b**+**c**), $\frac{1}{2}$ (**a**+**c**), $\frac{1}{2}$ (**a**+**b**) | 1 | $\Gamma_5^+\ (0,0,0)$ | 3 | $e_{xz}=e_{yz}=e_{xy}$ | |
| $Fd\bar{3}m(2)\rightarrow Cmca(4)$ | □→P I | $\frac{1}{2}$ (**b**−**a**), 2**c**, $\frac{1}{2}$ (**a**+**b**) | 1 | $\Gamma_5^+\ (0,0,0)$ +$\Delta\ (0,0,\frac{\pi}{2c})$ +$Y_3^+\ (0,\frac{2\pi}{b},0)$ | 3<br>2<br><br>1 | $e_{xy}$, $e_{xz}=e_{yz}=0$ $\eta_1=\eta_2$<br>$\rho$ | $2e_{zz}-e_{xx}-e_{yy}$ |
| $Fm\bar{3}m(1)\rightarrow Cmca(8)$ | □→Bi IV | −2**c**, −**a**−**b**, **b**−**a** | 8 | $L_1^-\ (\frac{\pi}{a},\frac{\pi}{a},\frac{\pi}{a})$ +$Z_3^+\ (0,0,\frac{\pi}{c})$ | 4<br><br>1 | $\eta_1=\eta_2$, $\eta_3=\eta_4=0$<br>$\rho$ | $2e_{zz}-e_{xx}-e_{yy}$ |

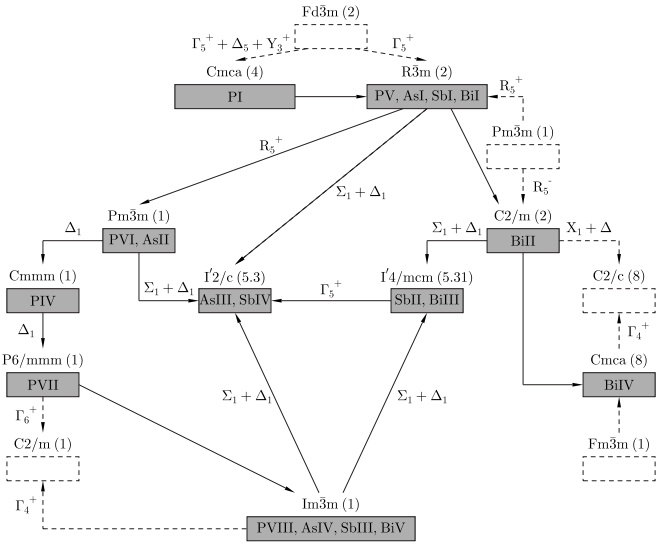


FIG. 15. Symmetry relationship between the structures observed in Group Va elements. Hypothetical structures assuming the role of intermediate (or parent) phases in the proposed structural mechanisms are indicated by white boxes. The irreducible representations associated with the symmetry-breaking mechanisms are indicated along the lines relating the structures. The arrows are oriented from the initial to final structures as in Table I. The full notation of the superspace groups $I'4/mcm$ and $I'2/c$ is given in the text.

ondary order parameter coupled to the primary $R_5^+$ instability. It has to be noted that the first-order character of the A7-pc transition is imposed by the property of the secondary order parameter, which transforms as the $\Gamma_5^+$ zone-center IR, to allow the cubic invariant $e_{yz}e_{xz}e_{xy}$ in the transition free energy, while the primary (symmetry breaking) $\eta_i$ order parameter allows the transition to be second order. The pc structure is stabilized in P and As, whereas in Sb and Bi, it is approached but not realized, as attested by the observation in these two elements of a steady increase with pressure of the rhombohedral angle $\alpha$ which reaches a value close to 60° or, equivalently, of a decrease of the $c/a$ ratio (in the hexagonal setting) down to the near limit of $c/a=\sqrt{6}$. In Bi, the A7 structure transforms into the monoclinic Bi II structure induced by another three-dimensional IR of the pc Brillouin zone $(R_5^-)$ corresponding to the same $R$ point which yields the A7 structure.

Raman scattering experiments have confirmed accurately the role played by the cubic $R$-point instability in the structural path of As, Sb, and Bi.[27,31,44,45] In the A7 structure, the cubic $R_5^+$ mode splits into two zone-center $\Gamma$ optical modes: a singly degenerated totally symmetric $\Gamma_1^+$ $(A_{1g})$ mode and a doubly degenerated $\Gamma_3^+$ $(E_g)$ mode, representing, respectively, displacements along the $C_3$ axis and in the perpendicular direction. The two modes have been found to soften on approaching the higher-pressure transitions. In As,[27] the softening is by 17% and 30% for $\Gamma_1^+$ and $\Gamma_3^+$, and in Sb (Refs. 31 and 45) by about 20% for both modes. In Sb, Wang *et al.*[31] observed a hardening of the modes in the host-guest Sb II-Sb IV pressure region and indications, prior to the Sb I→Sb IV transition, of a coupling of the zone-center optical modes to other phonon modes. These latter observations show that in Sb, our assumed shifting of the critical wave vector from the $R$ point along the $\Theta$ $\left(\frac{2\pi}{7a},\frac{2\pi}{7a},k_z\right)$ Brillouin-zone line occurs just before the onset of a latent cubic structure.

### B. Different structural paths from the primitive cubic to bcc structures

Therefore, the transition sequences found in the four elements can be considered as intermediate structural paths for achieving under pressurization the pc-to-bcc reconstructive mechanism. Calcium is the only known example of material in which this mechanism occurs directly[43] in the reversed sense with respect to Group Va elements, i.e., from a lower-pressure bcc structure with a closer packing fraction of atoms (0.680) to a more open higher-pressure pc structure having a lower packing fraction of 0.524. In elements of Group Va, the indirect pc-to-bcc transformation follows a more standard scheme with a closer atomic packing at higher pressure. A number of different structural paths can be proposed for this transformation.

(1) The most direct path involves a compression of the pc structure along its body diagonal [111] with an increase of the rhombohedral angle $\alpha$ from 90° to 109.471°. Here, the spontaneous shear strains $e_{yz}=e_{xz}=e_{xy}$, which lower the pc symmetry to $R\bar{3}m$ $(Z=1)$, coincide with the primary order parameter. This highly reconstructive structural mechanism, which has been proposed for the 32 GPa transition in Ca,[13] is not observed in the Group Va elements.

(2) Another pc-to-bcc mechanism, shown in Figs. 11 and 12, proceeds via the monoclinic Bi II structure, which constitutes a common substructure to the pc and bcc structures. As indicated in Table I, the pc→Bi II group-subgroup related transition requires a zone-boundary instability $(R_5^-)$ supplemented by secondary strains $(e_{xy},2e_{zz}-e_{xx}-e_{yy})$. The Bi II-to-bcc group-subgroup related transition requires another zone-boundary instability $(H_4^-)$ with the same secondary strains. The Bi II-to-bcc transition can be realized across a tetragonally distorted bcc substructure of symmetry $I4/mmm$ $(Z=2)$, which gives rise to the host-guest Bi III and Sb II structures by the same displacive mechanism recently proposed for the formation of the Ba IV host-guest structure.[13] The slight monoclinic deformation of the tetragonal Sb II host-guest structure characterizing Sb IV and As III is reminiscent of the secondary strains arising at the monoclinic Bi II structure, which is skipped in Sb and As.

Accordingly, the host-guest structures found in As, Sb, and Bi can be interpreted in the framework of this second pc-to-bcc structural mechanism. The different structural sequences observed in the three elements relate to the different critical pressures at which the host-guest structures arise. In Bi, the lowest critical pressure of 2.8 GPa inhibits the formation of the cubic structure allowing instead a decomposition of the pc-to-bcc mechanism into two steps, with a narrow region of stability for the monoclinic structure. In As, in which the host-guest structure takes place at the highest critical pressure of 48 GPa, the pc structure is stabilized but the monoclinic-tetragonal stages are squeezed into a single frustrated monoclinic host-guest structure before the onset of the

bcc structure. Sb corresponds to an intermediate situation, the absence of a pc structure being compensated by a decomposition of the pc-to-bcc mechanism into two successive, monoclinic and tetragonal, host-guest structures.

It remains to be understood why the frustrated composite host-guest structures are favored with respect to the sequence of commensurate $C2/m$-$I4/mmm$ structures assumed in the considered pc-to-bcc transformation mechanism. Both the Bi II and the host-guest structures of Bi III can be considered as real intermediate stages in the pc-to-bcc transition mechanism which involves an increase of the interatomic distances and the coordination number of the atoms from 6+12 in the simple cubic to 8+6 in the bcc structure. At the A7 → Bi II transition, the coordination number of the bismuth atoms changes from 6+12 to 6+3+9. In the structure of Bi III, the host atoms have CN 8 (6 host atoms +2 guest atoms), whereas the coordination number of the guest atoms ranges from CN 6 (guest atoms located in the center of the squares) to CN 10 (guest atoms located in the center of the antiprisms). Accordingly, the composite character with a modulation of the host atoms within the $x/y$ plane and the guest atoms along $c$ facilitates a continuous adjustment of the interatomic distances and the resulting coordination number, allowing the reconstructive mechanism to take place in a less abrupt way than the commensurate $C2/m$-$I4/mmm$ path.

(3) A further different structural path, shown in Figs. 6 and 7, relates the pc and bcc structures in phosphorus. As already noted, the basic commensurate orthorhombic *Cmmm* unit cell of the incommensurate P IV structure represents the maximal intermediate common substructure to the pc P VI and primitive hexagonal (ph) P VII structures. The P VI → P IV and P IV → P VII ferroelastic transitions correspond, respectively, to the primary order-parameter strains $e_{xy}$ and $e_{xx}-e_{yy}$. The wave number of the incommensurate modulation found along the P IV $c$ axis[4] coinciding with the hexagonal $c$ direction decreases slightly from 0.268 to 0.266 between 113 and 137 GPa. In the same pressure range, the P IV lattice parameters $a$, $b$, and $c$ shrink, respectively, by only 1.5%, 0.2%, and 1.2%.[4] In contrast, drastic structural changes occur at the P VI → P IV and P IV → P VII transitions, the $\gamma$ angle of a corresponding primitive monoclinic unit cell jumping discontinuously from 90° to 97.8° and from 99° to 120°, respectively. Such behavior is imposed by the necessity to transform the pc configuration into the ph one in the relatively narrow stability range of pressure (30 GPa) of the P IV structure. The abrupt character of the strongly first-order P VI → P IV transition at 107 GPa, with a volume reduction of 2.6%, differs from the continuous behavior usually found at transitions to incommensurate structures. It denotes a lock-in-type behavior, consistent with the almost constant value of the modulation wave number within the P IV pressure range. At variance, the 137 GPa first-order volume discontinuity of 5.5% which ends the incommensurate regime corresponds to a standard lock-in transition to the commensurate ph P VII structure. One should explain why the system prefers an incommensurate path between the pc and ph structures instead of the commensurate *Cmmm* common substructure. The pc-to-ph transition involves a change of the coordination number from 6 to 8 with an increase of the average interatomic distance by about 2.5%. A comparison of the P IV structure with the nonmodulated *Cmmm* structure shows that *the incommensurability is necessary to preserve the interatomic distances in the first coordination sphere*, making the incommensurate path energetically more favorable than the commensurate path despite the occurring atomic displacements.

The P VII → P VIII transition proceeds via an underlying monoclinic substructure which separates two ferroelastic distortions: a shear strain $e_{yz}$ lowers the ph symmetry to monoclinic $C2/m$, followed by another shear strain $e_{yz}=e_{xz}$ which increases the monoclinic symmetry to bcc. The relatively small volume drop reported for the corresponding reconstructive mechanism (2.8%) (Ref. 26) results from the extremely high transition pressure (262 GPa), the bcc volume at 280 GPa being already reduced to 37.3% of the ambient pressure volume.[26]

The different pc-to-bcc structural path followed in phosphorus with respect to the other Group Va elements is related to the wide range of stability of the P VI structure which extends from 10.2 to 107 GPa. Within this interval, the lattice parameters steadily decrease with a lowering of the atomic volume[22] from 13.606 to 9.601 Å$^3$. Therefore, the structural instabilities activated on approaching the high-pressure limit should lead to structures with a higher packing fraction of atoms and higher coordination numbers, such as the ph structure whose packing fraction (0.605) is midway between the pc and bcc packing fractions and corresponds to an increase of the coordination number from 6 to 8.

### C. Comparison with the current theoretical analysis of the evolution of the electronic configuration of Group Va elements under pressure

It is desirable to compare our analysis of the structural mechanisms associated with the high-pressure polymorphism in Group Va elements with the theoretical picture assumed for the evolution of their electronic configuration under pressure. Group Va has the defining characteristic that all the component elements have five electrons in their outmost shell, that is, two electrons in the $s$ subshell and three unpaired electrons in the $p$ subshell. In the A7 structure, the three $p$ electrons form covalent bonds with the $p$ electrons of the nearest neighbors. Due to the bonding $p$-$p$ orbitals, the three states are fully occupied, whereas the antibonding $p$-$p$ states are empty. This gives a semiconductor at ambient condition. With increasing pressure and smaller atomic volumes, the amount of overlap between the $s$ and $p$ states gets larger and structures with higher coordination become possible, the $s^2p^3$ bonding favoring bond angles close to 90°. Therefore, the A7-to-pc transition is interpreted[46,47] as a prototype example of a pressure-induced first-order transformation[48] of a Peierls distorted semiconductor into an elemental metal due to the overlap of the $s$-$p$ orbitals, the reverse rhombohedral distortion opening a gap at the Fermi level and lowering the band contribution to the total energy.

At moderate compression, *ab initio* density functional calculations[12] show that the emergence of the host-guest structures in As, Sb, and Bi cannot be explained by a pressure-induced change in their valence state and should be

interpreted as the result of a lowering of the energy band contribution to the total energy with an increasing contribution of the electrostatic Madelung energy. The stability of the host-guest structures should reflect an interplay between almost equal amounts of the two contributions to the total energy, with an average coordination number varying between 7 and 9, midway between the pc and bcc structures. At the highest pressures attained for the three elements, the stability of the bcc structure is governed by the electrostatic contribution, the valence state remaining unchanged, with a still significant presence of covalent bonding. In the pressure range of the pc and ph structures, phosphorus should differ from its heavier congeners[49] by the disappearance of the bonding-antibonding splitting, a strong overlapping of the *s* and *p* bands, and an increased *d*-state filling of the occupied bands. The tendency of the lighter element to undergo *s*-*d* transition associated with a subsequent hybridization at higher pressure explains its different structural sequence and especially the simple ph structure that should be stabilized by the admixture of *d* state. Therefore, at variance with As, Sb, and Bi, the P VI-P IV-P VII sequence is interpreted as electronically driven, up to the bcc P VIII structure which is governed by electrostatic interactions.

Electronic considerations provide a decisive argument for explaining why the lower-symmetry A7 structure occurs at lower pressure than the higher-symmetry pc structure, in contrast to the usual trend observed for pressure-induced phase transitions where the parent structure is generally stabilized at lower pressure.[13,14,18] The *ab initio* interpretation of the host-guest structures and P IV-P VII structural sequence as different intermediate stages between the open pc and closer packed bcc structures is consistent with our proposed structural arguments. However, the qualitative description of the host-guest structures as energetically frustrated states due to a delicate balance between two distinct contributions to the total energy is at variance with our description in terms of a structural frustration required to facilitate the A7-to-bcc reconstructive mechanism. On the other hand, the recently disclosed incommensurate character of the P IV structure,[4] not considered in Ref. 49, sheds a new light on the sequence of transitions in phosphorus, showing that a structural frustration also occurs in the lighter Group Va element. The structural sequence occurring in phosphorus may be related to the *s*-*d* transfer found by *ab initio* calculations, but also to another structural route on the way to the bcc structure, that would not require substantial change in the electronic configuration but correspond to a set of displacements energetically more favorable at very high pressures.

## IV. SUMMARY AND CONCLUSION

In summary, the high-pressure phase transitions in the four considered Group Va elements have been described in terms of displacive atomic mechanisms. Except for the A7 $\rightarrow$pc transition, all structural mechanisms display a reconstructive character, which requires going through hypothetical intermediate structures which may be tested as representing the minimal energy paths in total energy calculations. Two different structural sequences are proposed to relate the A7 low-pressure structure to the bcc high-pressure structure. (1) One structural sequence available for the heavier elements As, Sb, and Bi goes across the monoclinic Bi II structure and a body-centered tetragonal substructure, from which the formation of the host-guest and bcc structures can both be derived via small displacements. The incommensurate character of the host-guest structures is interpreted as resulting from a continuous adjustment of interatomic distances which allows the coordination number to increase smoothly toward the bcc configuration. Different structural mechanisms have been proposed[13,14] for the formation of the host-guest structures reported in Groups Ia (Refs. 6 and 7) and IIa (Refs. 8 and 9) elements. However, it can be noted that these mechanisms involve the same underlying tetragonal $I4/mmm$ substructure[13,14] used as an intermediate path in the reconstructive processes leading to the host-guest structures in Group Va. This may explain the apparent structural similarity of the host-guest structures in elemental groups displaying different chemical bonding and electronic structures. (2) Another structural path is followed in P going through the commensurate P IV subcell and a monoclinic substructure relating P VII and P VIII. Here, again, the incommensurate character of the P IV structure is interpreted as resulting from the minimal energy rule characterizing the real path followed between two structures separated by a reconstructive phase transition.

A number of features of the high-pressure polymorphism in Group Va have been noted as reminiscent of Group IVa polymorphism. Thus, the P VII structure has the primitive hexagonal symmetry found among elements only for Si V and Ge V, and the orthorhombic Bi IV structure is isostructural with Si VI and Ge VI. The highest-pressure bcc structure of Group IVa is also the highest-pressure structure for Sn and Pb. The black phosphorus P I and A7 structures have been shown in Sec. II to derive from the diamond-type structure present in all Group IVa elements except Pb. On the other hand, the room-pressure structure of the Group VIa element Po is primitive cubic[5] and the coordination in amorphous As is threefold, structurally intermediate between tetrahedrally coordinated Group IVa amorphous films of Si and Ge and the twofold coordination of the chalcogenide glasses of Group VIa elements S, Se, and Te.[50] This structural continuity in the polymorphism of the three groups also appears in their common tendency toward lower transition pressures for the heavier members of the group. It has been suggested[5] to be related to the covalent bonding and the strong electron correlation in the valence band, which are common features of the three groups, but it still remains to be understood theoretically.

*hanne@min.uni-kiel.de

[1] M. I. McMahon, O. Degtyareva, and R. J. Nelmes, Phys. Rev. Lett. **85**, 4896 (2000).
[2] O. Degtyareva, M. I. McMahon, and R. J. Nelmes, Phys. Rev. B **70**, 184119 (2004).
[3] M. I. McMahon, O. Degtyareva, R. J. Nelmes, S. van Smaalen, and L. Palatinus, Phys. Rev. B **75**, 184114 (2007).
[4] H. Fujihisa, Y. Akahama, H. Kawamura, Y. Ohishi, Y. Gotoh, H. Yamawaki, M. Sakashita, S. Takeya, and K. Honda, Phys. Rev. Lett. **98**, 175501 (2007).
[5] D. A. Young, *Phase Diagrams of the Elements* (University of California Press, Berkeley, 1991).
[6] M. I. McMahon, S. Rekhi, and R. J. Nelmes, Phys. Rev. Lett. **87**, 055501 (2001).
[7] M. I. McMahon, R. J. Nelmes, U. Schwarz, and K. Syassen, Phys. Rev. B **74**, 140102(R) (2006).
[8] M. I. McMahon, T. Bovornratanaraks, D. R. Allan, S. A. Belmonte, and R. J. Nelmes, Phys. Rev. B **61**, 3135 (2000).
[9] R. J. Nelmes, D. R. Allan, M. I. McMahon, and S. A. Belmonte, Phys. Rev. Lett. **83**, 4081 (1999).
[10] H. Fujihisa, Y. Akahama, H. Kawamura, Y. Gotoh, H. Yamawaki, M. Sakashita, S. Takeya, and K. Honda, Phys. Rev. B **72**, 132103 (2005).
[11] S. K. Reed and G. J. Ackland, Phys. Rev. Lett. **84**, 5580 (2000).
[12] U. Häussermann, K. Söderberg, and R. Norrestam, J. Am. Chem. Soc. **124**, 15359 (2002).
[13] H. Katzke and P. Tolédano, Phys. Rev. B **75**, 174103 (2007).
[14] H. Katzke and P. Tolédano, Phys. Rev. B **71**, 184101 (2005).
[15] P. Tolédano and V. Dmitriev, *Reconstructive Phase Transitions* (World Scientific, Singapore, 1996).
[16] J. Donohue, *The Structures of the Elements* (Wiley, New York, 1974).
[17] A. Morita, Appl. Phys. A: Solids Surf. **39**, 227 (1986).
[18] H. Katzke, U. Bismayer, and P. Tolédano, Phys. Rev. B **73**, 134105 (2006).
[19] S. Sugai, T. Ueda, and K. Murase, J. Phys. Soc. Jpn. **50**, 3356 (1981).
[20] J. K. Burdett and S. Lee, J. Am. Chem. Soc. **105**, 1079 (1983).
[21] T. Kikegawa and H. Iwasaki, Acta Crystallogr., Sect. B: Struct. Sci. **39**, 158 (1983).
[22] Y. Akahama, M. Kobayashi, and H. Kawamura, Phys. Rev. B **59**, 8520 (1999).
[23] R. Ahuja, Phys. Status Solidi B **235**, 282 (2003).
[24] F. J. H. Ehlers and N. E. Christensen, Phys. Rev. B **69**, 214112 (2004).
[25] T. Ishikawa, H. Nagara, K. Kusakabe, and N. Suzuki, Phys. Rev. Lett. **96**, 095502 (2006).
[26] Y. Akahama, H. Kawamura, S. Carlson, T. Le Bihan, and D. Häusermann, Phys. Rev. B **61**, 3139 (2000).
[27] H. J. Beister, K. Strössner, and K. Syassen, Phys. Rev. B **41**, 5535 (1990).
[28] O. Degtyareva, M. I. McMahon, and R. J. Nelmes, High Press. Res. **24**, 319 (2004).
[29] S. van Smaalen, Crystallogr. Rev. **4**, 79 (1995).
[30] R. G. Greene, H. Luo, and A. L. Ruoff, Phys. Rev. B **51**, 597 (1995).
[31] X. Wang, K. Kunc, I. Loa, U. Schwarz, and K. Syassen, Phys. Rev. B **74**, 134305 (2006).
[32] T. N. Kolobyanina, S. S. Kabalkina, L. F. Vereshchagin, and L. V. Fedina, Sov. Phys. JETP **28**, 88 (1969).
[33] K. Aoki, S. Fujiwara, and M. Kusakabe, Solid State Commun. **45**, 161 (1983).
[34] R. M. Brugger, R. B. Bennion, and T. G. Worlton, Phys. Lett. **24A**, 714 (1967).
[35] L. G. Akselrud, M. Hanfland, and U. Schwarz, Z. Kristallogr. - New Cryst. Struct. **218**, 415 (2003).
[36] J. H. Chen, H. Iwasaki, and T. Kikegawa, High Press. Res. **15**, 143 (1996).
[37] E. M. Compy, J. Appl. Phys. **41**, 2014 (1970).
[38] K. Aoki, S. Fujiwara, and M. Kusakabe, J. Phys. Soc. Jpn. **51**, 3826 (1982).
[39] Y. Akahama, H. Kawamura, and A. K. Singh, J. Appl. Phys. **92**, 5892 (2002).
[40] J. H. Chen, H. Iwasaki, and T. Kikegawa, J. Phys. Chem. Solids **58**, 247 (1997).
[41] V. F. Degtyareva, Phys. Rev. B **62**, 9 (2000).
[42] The notation of the irreducible representations is that of Stokes and Hatch for the points of the Brillouin-zone surfaces and for the Brillouin-zone center [H. T. Stokes and D. M. Hatch, *Isotropy Space Groups of the 230 Crystallographic Space Groups* (World Scientific, Singapore, 1988)]. For the points, lines, and surfaces inside the Brillouin zone, the notation of Zak *et al.* is used [J. Zak, A. Cacher, H. Glück, and Y. Gur, *Irreducible Representations of Space Groups* (Benjamin, New York, 1969)].
[43] H. Olijnyk and W. B. Holzapfel, Phys. Lett. **100A**, 191 (1984).
[44] W. Richter, T. Fjeldly, J. Renucci, and M. Cardona, in *Proceedings of the International Conference on Lattice Dynamics, Paris*, edited by M. Balkanski (Flammarion, Paris, 1978), p. 104.
[45] O. Degtyareva, V. V. Struzhkin, and R. J. Hemley, Solid State Commun. **141**, 164 (2007).
[46] M. H. Cohen, L. M. Falicov, and S. Golin, IBM J. Res. Dev. **8**, 215 (1964).
[47] K. J. Chang and M. L. Cohen, Phys. Rev. B **33**, 7371 (1986).
[48] A. A. Abrikosov and L. A. Falkovskii, Sov. Phys. JETP **16**, 769 (1963).
[49] U. Häussermann, Chem.-Eur. J. **9**, 1472 (2003).
[50] G. E. Jellison, Jr., G. L. Petersen, and P. C. Taylor, Phys. Rev. Lett. **42**, 1413 (1979).